The 2025 World Congress on
Advances in Structural Engineering and Mechanics (ASEM25)
BEXCO, Busan, Korea, August 11-14, 2025

Temperature-dependent electrodeposition behavior in seawater-saturated sand

*Ba-Da Lee$^{1)}$ and Yeong-Man Kwon$^{2)}$

1), 2) Department of Civil Engineering, Pukyong National University, Pusan 48513, Korea
1) js12023@pknu.ac.kr
2) yeongman.kwon@pknu.ac.kr

ABSTRACT

Soil electrodeposition is an emerging ground improvement technique that induces mineral precipitation by electrically activating dissolved ions in groundwater. This electrochemical process improves soil properties while minimizing the use of chemical additives and energy during treatment. To deepen insight into electrodeposition under in-situ marine conditions, this study utilized seawater from the Gwangalli coast in Busan, Korea, and introduced temperature variations (5, 20, and 30 °C) to replicate key environmental factors encountered in the field. Laboratory tests using custom-designed electrochemical cells were conducted to investigate the temperature-dependent nucleation and growth of electrodeposits. The results confirmed that electrodeposition occurred consistently across all temperature ranges, indicating its feasibility under realistic marine conditions. A more detailed analysis, however, revealed that temperature plays a key role in electrochemical behavior; higher temperatures increased current flow, decreased electrical resistance, and accelerated mineral precipitation. These findings validate the applicability of electrodeposition in coastal settings and offer valuable insights for the development of sustainable ground improvement techniques in coastal and underground construction.

1. INTRODUCTION

Human populations are densely concentrated along shorelines, with nearly half of the urban population residing within 100 km of the coastal area (Barragán & de Andrés, 2015). Continued growth of urbanization in these regions necessitates infrastructure expansion to accommodate increasing population densities and economic activities (Hanson et al., 2010). However, saturated soil layers, commonly found in coastal zones,

---

[1)] Undergraduate Student
[2)] Assistant Professor

are inherently weak due to their high water content, making them susceptible to collapse (Mitchell, 1976). Consequently, these conditions pose significant geotechnical risks, including erosion and instability. Conventional ground improvement methods such as grouting and chemical injection have been employed to enhance soil strength (Spagnoli, 2021; Verma et al., 2021). However, these methods typically require substantial energy input and involve chemical agents that present environmental risks, including toxicity and potential groundwater contamination (Walker et al., 1997). Furthermore, their effectiveness in highly permeable sandy soils is often limited due to difficulties in achieving uniform treatment (Suelen da Rocha Gomes, 2023) .

To address these challenges, this study examines soil electrodeposition as a sustainable alternative for coastal ground improvement. Electrodeposition is an electrochemical process that induces the precipitation of mineral binders such as magnesium hydroxide ($Mg(OH)_2$) and calcium carbonate ($CaCO_3$) through the application of a mild electric potential between electrodes immersed in ion-rich seawater. This technique promotes the precipitation of mineral binders at soil particle contacts, enhancing particle bonding without requiring external chemical injections, thus reducing both energy consumption and environmental impacts (Devi et al., 2024). In detail, this study evaluates the feasibility and practical applicability of electrodeposition under realistic marine conditions by utilizing natural seawater at varying temperature scenarios.

Laboratory-scale soil electrodeposition experiments were conducted using Jumunjin standard sand and seawater collected from Gwangalli Beach, Busan, Korea. Tests were performed under constant voltage conditions (i.e., 2, 3, and 4 V) and at controlled temperatures (i.e., 5, 20, and 30 °C) for a duration of 7 days. The efficiency of electrodeposition process was quantitatively assessed by monitoring electric current, identifying precipitated mineral phases, and quantifying the volume of mineral deposits. Through these controlled laboratory experiments, the applicability of electrodeposition as a sustainable ground improvement technique under realistic marine conditions was systematically investigated.

2. General chemical reaction

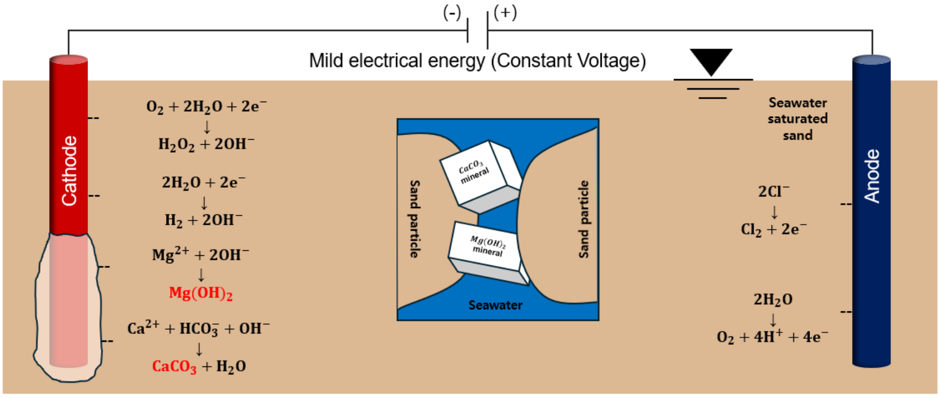

Fig 1. Schematic representation of electrochemical precipitation for soil improvement.

Electrodeposition-based soil stabilization relies on electrochemical reactions that promote the precipitation of mineral binders within the soil matrix when an electric potential is applied between electrodes embedded in saturated soils (Devi et al., 2024). This process leads to enhanced soil strength and stability through the generation of cementing materials (i.e., $Mg(OH)_2$ and $CaCO_3$).

At the cathode, hydroxide ions (OH^-) are primarily generated through two distinct electrochemical pathways depending on the applied voltage. At relatively lower voltages, the oxygen reduction reaction predominates as:

$$\mathrm{O_2 + 2H_2O + 2e^- \rightarrow H_2O_2 + 2OH^-} \qquad (1)$$

At higher voltages, the water reduction reaction (WRR) becomes dominant emitting hydrogen gas as:

$$\mathrm{2H_2O + 2e^- \rightarrow H_2 + 2OH^-} \qquad (2)$$

The generated OH^- ions subsequently react with magnesium and calcium ions naturally present in seawater, resulting in precipitation of $Mg(OH)_2$ and $CaCO_3$ as:

$$\mathrm{Mg^{2+} + 2OH^- \rightarrow Mg(OH)_2} \qquad (3)$$

$$\mathrm{Ca^{2+} + HCO_3{}^- + OH^- \rightarrow CaCO_3 + H_2O} \qquad (4)$$

On the anode side, electrochemical reactions involve the oxidation of water and chloride ions present in seawater, resulting in the production of electrons as:

$$\mathrm{2Cl^- \rightarrow Cl_2 + 2e^-} \qquad (5)$$

$$\mathrm{2H_2O \rightarrow O_2 + 4H^+ + 4e^-} \qquad (6)$$

3. Materials & Methods

3.1 Soil: Jumunjin standard sand

This study used standard sand, obtained from Jumunjin, Republic of Korea. The sand was classified as poorly graded sand (SP) (ASTM D2487-23), with a coefficient of uniformity (C_u) of 1.43 and a coefficient of gradation (C_c) of 0.93. The grain size distribution curve of the sand is presented in Figure 2.

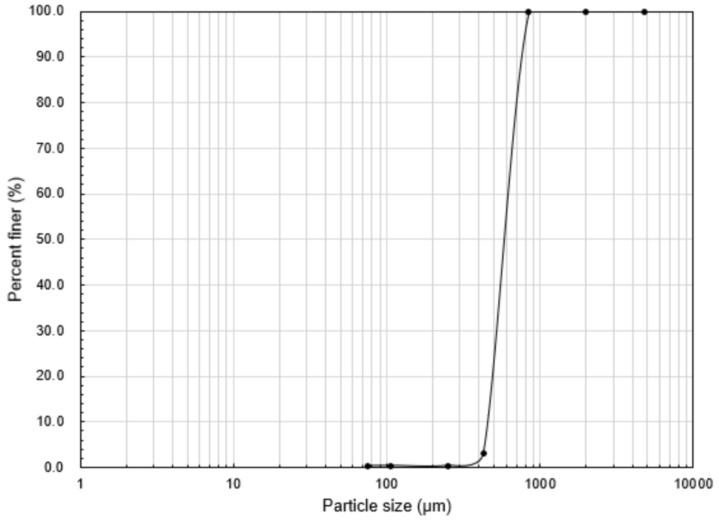

Figure 2. Particle size distribution of Jumunjin sand.

3.2 Seawater: Natural seawater collected from Gwangalli beach, Busan, Korea

Natural seawater used in this experiment was collected from Gwangalli beach, Busan, Korea (Coordinates: 35° 9′ 2.71″ N, 129° 7′ 0.58″ E; WGS84). Ion chromatography analysis (Aquion, Thermo Fisher Scientific Inc., US) of the seawater indicated the presence of the major cations including Na^+, Mg^{2+}, and Ca^{2+}, as shown in Fig. 3a. The seawater obtained from Gwangalli Beach contained higher concentrations of Ca^{2+} and Mg^{2+} ions compared to standard seawater (ASTM D1141-98; Fig. 3b). This elevated ionic concentration is likely due to the shallow coastal environment, characterized by sediment-water interactions, evaporation-driven ion enrichment, active biological processes, and terrestrial input (Lebrato et al., 2020). Since Ca^{2+} and Mg^{2+} are key ions in electrodeposition reactions, their higher availability in coastal seawater suggests potentially improved effectiveness of electrochemical soil stabilization methods in coastal regions compared to open ocean conditions.

Table 1. Ion composition of seawaters

Ion type	Gwangalli seawater (g/L)	Standard seawater (g/L)
Na^+	9.04	10.56
NH_4^+	0.80	-
K^+	0.37	0.38
Mg^{2+}	3.34	1.26
Ca^{2+}	1.10	0.4
PO_4^{3-}	0.69	-
Cl^-	20.97	18.98

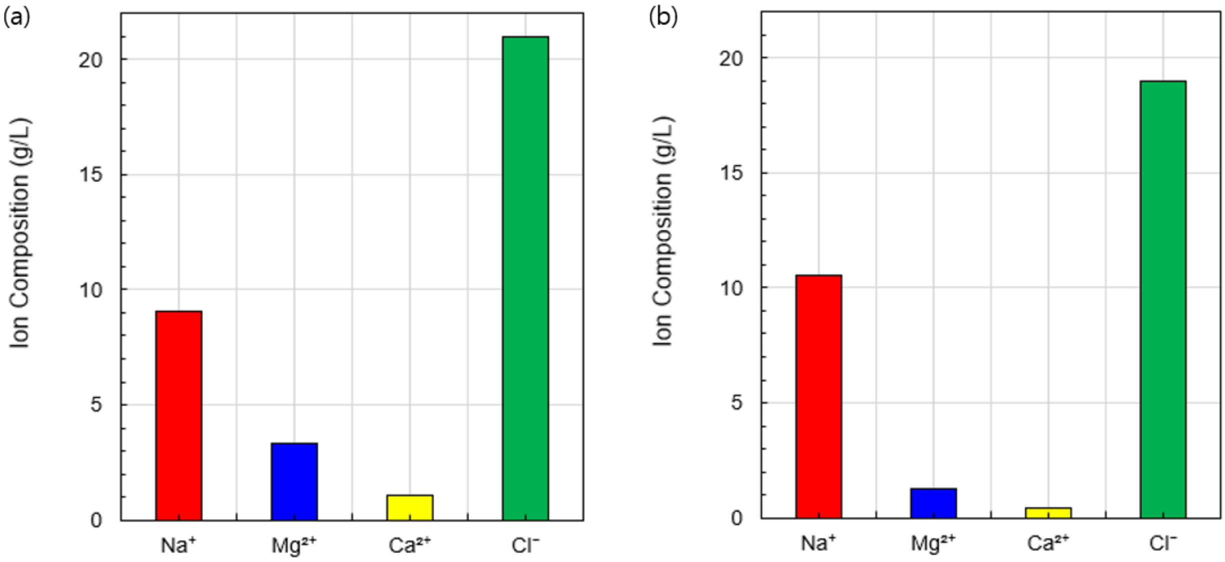

Figure 3. Ion composition of seawater sampled from (a) Gwangalli seawater and (b) Standard seawater

3.3. Electrodeposition equipment

This study utilized a distinct electrodeposition setup (Fig. 4) designed to investigate the temperature-dependent mechanisms of electrodeposition in soils. Sand specimens were prepared to achieve a dry density of 1.41 ± 0.03 g/cm³ and subsequently saturated with seawater collected from Gwangalli. Then, electrodes and a temperature sensor were properly inserted into the soil specimens. The cathode used in the experiments was stainless steel 304 (Steel&I, Korea), with a diameter of 2 mm and a submerged depth of 70 mm. In each experiment, the anode was made of platinum (Made lab, Korea), with a diameter of 1 mm and the same submerged depth as the cathode. The electrodes were positioned 70 mm apart. The temperature measuring instrument (HI10530; Hanna Instruments Inc., Woonsocket, RI, USA) was placed between the cathode and the anode to monitor temperature over time. The specimens were subjected to constant voltages of 2, 3, and 4 V, supplied by a direct-current power controller (2280S-32-6; Keithley Instruments, Cleveland, OH, USA).

3.4. Measurement of mass of electrodeposits

The mass of electrodeposits formed under different constant voltage (i.e., 2, 3, and 4 V) and temperature (i.e., 5°C, 20°C, and 30°C) conditions was measured using a precise scale (CBL-3200, CAS Corporation, Korea). To ensure accurate mass determination, the electrodeposits were air-dried for 3 days after 7 days of the experimental period. The net mass of the electrodeposits was calculated from the difference in electrode mass measured before and after the precipitation process.

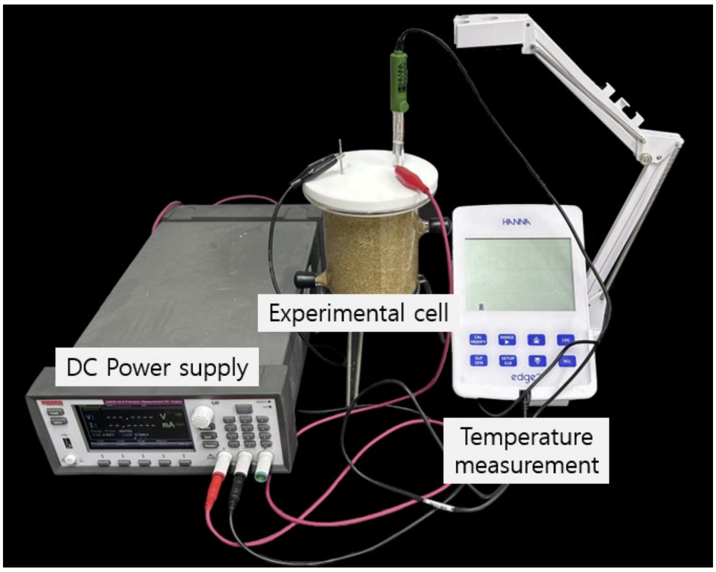

Figure 4. Electrodeposition set-ups

3.5. Microscopic observations

Scanning electron microscopy (SEM) analysis were conducted using a field emission SEM (MAGNA, TESCAN, Czech Republic). The specimens were air-dried thoroughly, and carefully mounted on an SEM stub using double-sided carbon tape prior to analysis. The specimen was coated with a platinum layer under vacuum conditions using a sputter coater operated at a current of 10 mA for 30 seconds to enhance surface conductivity for SEM imaging.

4. Results and analysis

4.1. Generals in electrodeposited mineral binders

The formation of mineral binders within the soil matrix as a result of electrodeposition was confirmed through SEM observations, as shown in Fig. 5. In Fig. 5a, mineral precipitates are visibly deposited between sand particles, coating their surfaces, and effectively binding them together. These mineral coatings appear to fill the voids between particles and serve as cementing agents, contributing to the structural integrity of the treated soil by enhancing interparticle bonding.

Figure 5b presents high-magnification SEM images that highlight the morphological diversity of the precipitated minerals. Various crystal forms were identified, including polymorphs of $CaCO_3$, namely calcite, aragonite, and vaterite, as well as brucite, representing $Mg(OH)_2$. Calcite appeared as rhombohedral crystals, aragonite showed needle-like radiating clusters, and vaterite exhibited spherical or cauliflower-shaped aggregates. Brucite formed plate-like or net-like structures. This diversity in mineral morphology indicates the simultaneous precipitation of both Ca- and Mg-based minerals, suggesting that complex nucleation and growth mechanisms were at play under the applied electrochemical conditions in the seawater environment.

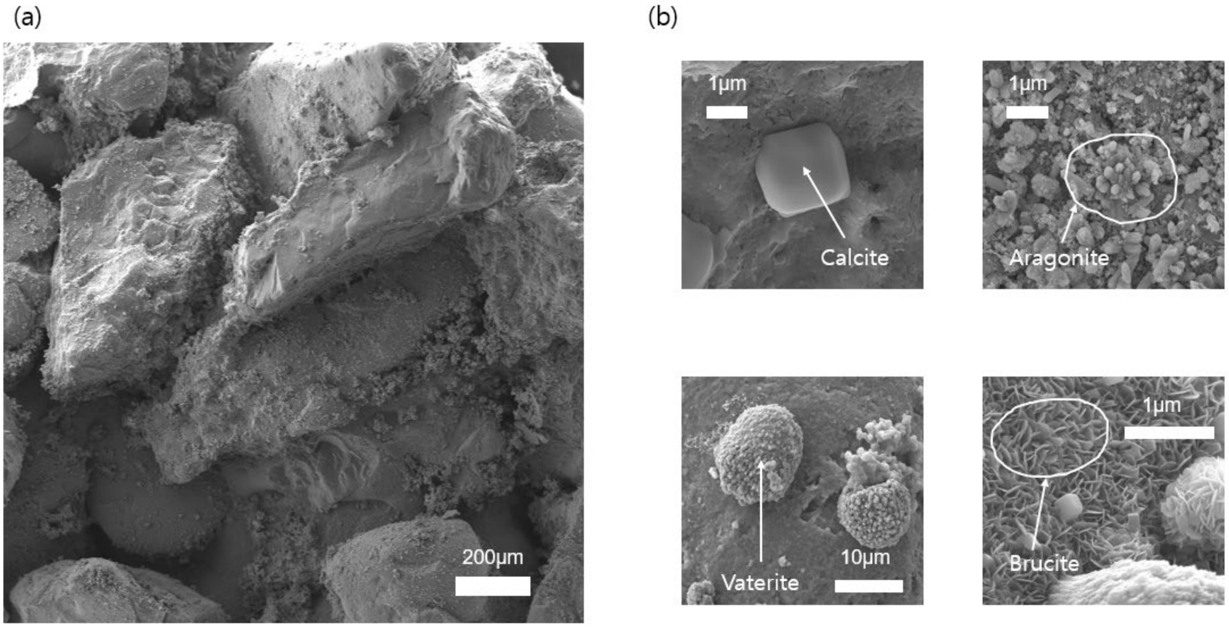

Figure 5. SEM images of mineral precipitates formed by electrodeposition under 3 V in Gwangalli seawater. (a) electrodeposit-induced soil cementation (b) specific mineral phases of rhombohedral calcite, needle-like aragonite, spherical vaterite, and plate-like brucite.

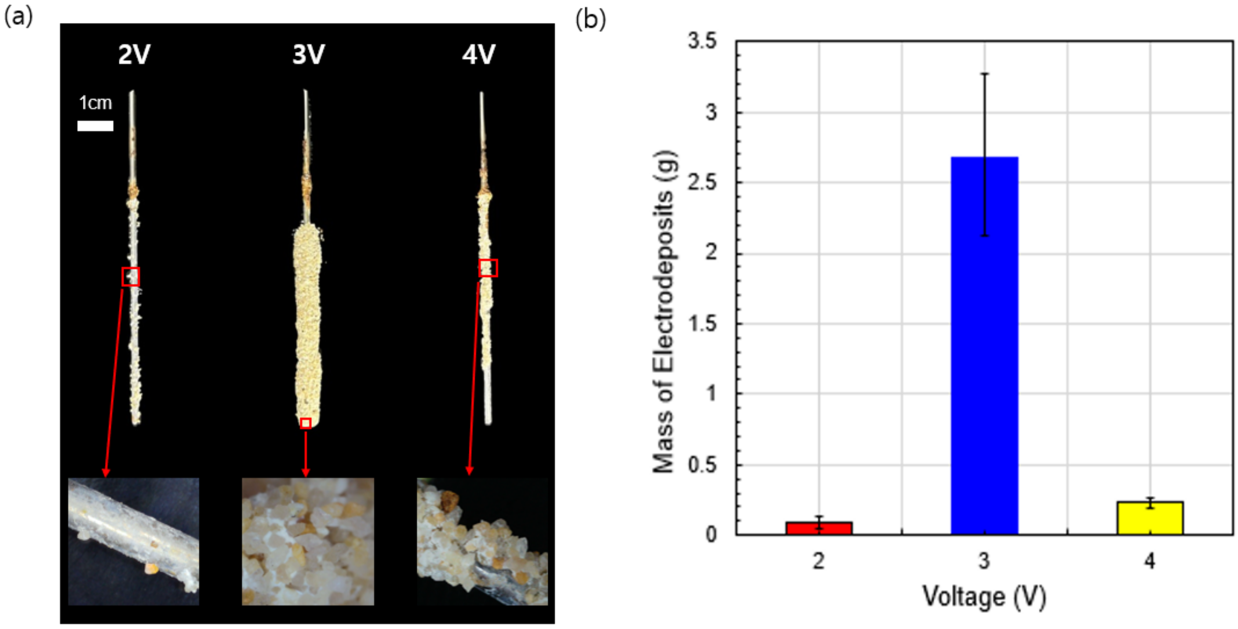

Figure 6. Effect of applied voltage on the formation of electrodeposits; (a) Visual comparison of mineral precipitation along electrodes subjected to 2 V, 3 V, and 4 V, with magnified views highlighting the extent and morphology of the deposits, and (b) the mass of electrodeposits formed at each voltage level.

4.2. Influence of applied voltage on electrodeposition

Figure 6 illustrates the effect of applied voltage on the formation of electrodeposits after 7 days of electrical stimulation. As shown in Fig. 6a, visually distinguishable white precipitates accumulated along the electrode, effectively cementing the surrounding sand particles. Notably, the density and coverage of electrodeposits varied significantly with the applied voltage.

Quantitative results in Fig. 6b show that the mass of electrodeposits peaked at 3 V, with significantly lower values at both 2 V and 4 V. At 2V, the relatively low energy input primarily favored the ORR to generate OH- ions near the cathode. However, the OH$^-$ concentration was insufficient to trigger substantial mineral precipitation, resulting in minimal electrodeposit formation. In contrast, while 4 V provided higher energy, it intensified the WRR, leading to hydrogen gas evolution (Lide & Frederikse, 1996). The generation of hydrogen gas bubbles dispersed the forming mineral phases away from the electrode vicinity, hindering their ability to nucleate and attach onto sand particles, thereby limiting effective coating and bonding.

These findings suggest that an applied voltage of 3 V offers a balanced electrochemical environment, promoting sufficient OH$^-$ generation without the destabilizing effects of intense gas evolution, thereby enabling optimal and stable electrodeposition. The resulting mineral precipitates play a key role in particle binding and the formation of a cemented soil matrix.

4.3. Temperature effect

As shown in Figure 7, both the morphology and mass of electrodeposits exhibit a positive dependence on temperature, underscoring the critical role of thermal conditions in the electrodeposition process. Visual inspection (Fig. 7a) reveals that the specimen treated at higher temperatures exhibited more extensive and continuous mineral accumulation along the electrode surface. In contrast, the specimen treated at lower temperatures showed sparse and uneven deposition.

Quantitative results in Fig. 7b further support this observation: the mass of electrodeposits increased from 1.2 g at 5 °C to 4.6 g at 30 °C. This increase in deposit coverage can be attributed to the temperature-dependent acceleration of ion mobility, electrochemical reaction kinetics, and mineral nucleation rates. Higher temperatures likely promote more efficient ion transport and supersaturation conditions near the electrode surface, facilitating the formation and growth of crystalline phases.

Overall, these findings highlight those elevated temperatures create more favorable thermodynamic and kinetic environments for mineral precipitation, leading to improved bonding potential and treatment efficiency in electrochemically stabilized soils.

The current–time profiles (Fig. 8) demonstrate a clear dependence of electrochemical behavior on temperature. Throughout the electrodeposition period, specimens subjected to higher temperatures exhibited consistently greater current magnitudes. Specifically, the current at 30 °C remained significantly higher than those at 20 °C and 5 °C, suggesting enhanced electrochemical activity under elevated thermal conditions.

This behavior can be attributed to increased ionic mobility and improved ion transport in the pore water at high temperatures, which facilitate faster charge transfer reactions at the electrode interface. As a result, both ionic conductivity and electrode kinetics are positively influenced, thereby accelerating the rate of mineral nucleation and growth. These electrochemical enhancements align with the increased mass of electrodeposits observed at higher temperatures, as shown in Fig. 7.

The gradually decreasing current over time, observed across all temperature conditions, reflects the progressive consumption of reactive ions and the formation of insulating mineral layers near the electrode. Nevertheless, the slower decay and higher steady-state current at elevated temperatures underscore the role of thermal energy in sustaining reaction rates. Collectively, these findings highlight temperature as a key operational parameter that governs the efficiency and effectiveness of electrodeposition-based soil improvement systems.

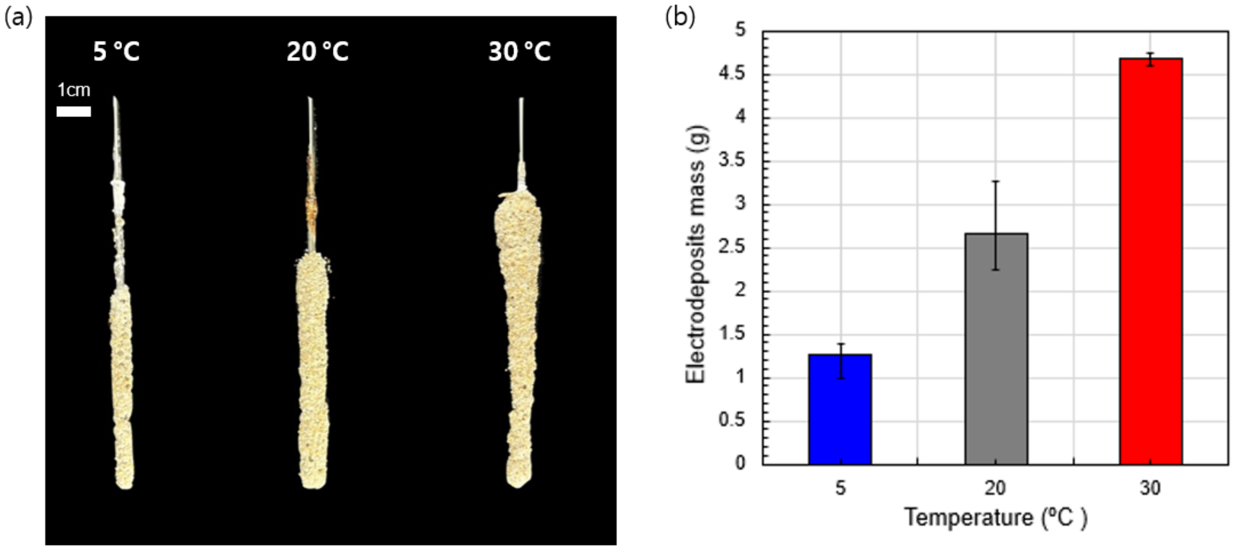

Figure 7. Effect of temperature on electrodeposition behavior; (a) Visual observation of electrodeposits formed at different temperatures (5 °C, 20 °C, and 30 °C) under a constant applied voltage of 3 V, and (b) the mass of electrodeposits formed after 7 days.

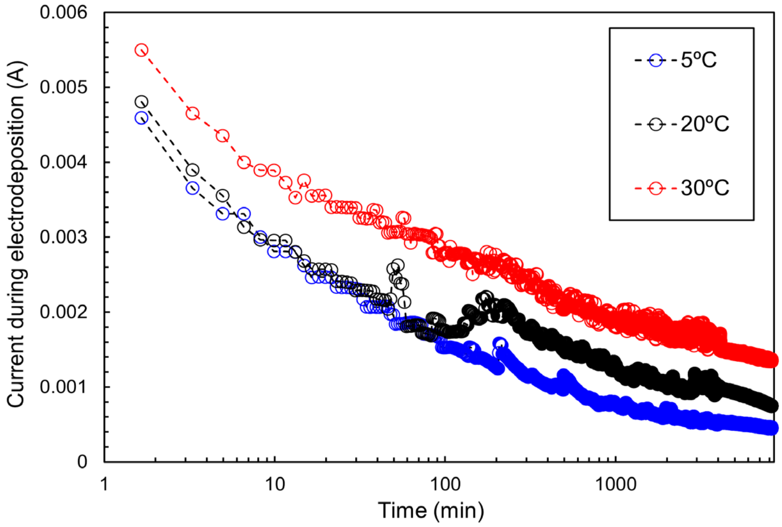

Figure 8. Effect of temperature on current evolution during electrodeposition.

5. Conclusions

This study evaluated the applicability of electrodeposition as an environmentally sustainable ground improvement method in coastal environments, focusing on the influence of temperature and voltage. Seawater-saturated Jumunjin sand was treated under varying temperatures (5, 20, and 30°C) and voltages (2, 3, and 4 V) for 7 days using natural Gwangalli seawater.

An applied voltage of 3V yielded the highest mass of mineral deposits, indicating an optimal balance between the oxygen reduction reaction (ORR) and the water reduction reaction (WRR). At lower voltage (2 V), low ionic mobility restricted mineral accumulation, whereas higher voltage (4 V) caused dominant water reduction reaction (WRR), increasing resistance and disturbing stable precipitation conditions. However, the long-term behavior of electrodeposition under higher voltages, particularly at 4 V, requires further investigation, as sufficient time may be necessary for mineral accumulation to occur over a broader soil volume.

The experimental results demonstrated that electrodeposition is thermally stable and effective across a wide temperature range, with significantly enhanced mineral accumulation at elevated temperatures. Higher temperatures improved ionic mobility and electrochemical kinetics, leading to increased current magnitudes and more effective mineral precipitation. Conversely, low temperatures resulted in reduced deposition efficiency due to limited ion activity.

These findings underscore the potential of electrodeposition as a low-impact, temperature-resilient soil stabilization method suitable for coastal infrastructure. Future research should focus on long-term field validation, performance under cyclic environmental loads, and optimization of electrode materials and system scalability.

Acknowledgements
This work was supported by the National Research Foundation of Korea (NRF) grant funded by the Korea government (MSIT) (RS-2025-00553627).

REFERENCES

ASTM. (2021). D1141-98: Standard Practice for Preparation of Substitute Ocean Water. In. West Conshohocken, PA: ASTM International.

Barragán, J. M., & de Andrés, M. (2015). Analysis and trends of the world's coastal cities and agglomerations. *Ocean & Coastal Management*, *114*, 11-20. https://doi.org/10.1016/j.ocecoaman.2015.06.004

Devi, N., Wagner, A., Lopez, J., Guerini, A., Zampini, D., & Rotta Loria, A. F. (2024). Mechanistic Insights into Electrodeposition in Seawater at Variable Electrochemical Potentials. *Advanced Sustainable Systems*, *8*(4), 2300446. https://doi.org/https://doi.org/10.1002/adsu.202300446

Hanson, S., Nicholls, R., Ranger, N., Hallegatte, S., Corfee-Morlot, J., Herweijer, C., & Chateau, J. (2010). A global ranking of port cities with high exposure to climate extremes. *Climatic change*, *104*(1), 89-111. https://doi.org/10.1007/s10584-010-9977-4

Lebrato, M., Garbe-Schonberg, D., Muller, M. N., Blanco-Ameijeiras, S., Feely, R. A., Lorenzoni, L., Molinero, J. C., Bremer, K., Jones, D. O. B., Iglesias-Rodriguez, D., Greeley, D., Lamare, M. D., Paulmier, A., Graco, M., Cartes, J., Barcelos, E. R. J., de Lara, A., Sanchez-Leal, R., Jimenez, P.,…Oschlies, A. (2020). Global variability in seawater Mg:Ca and Sr:Ca ratios in the modern ocean. *Proceedings of the National Academy of Sciences of the United States of America*, *117*(36), 22281-22292. https://doi.org/10.1073/pnas.1918943117

Lide, D. R., & Frederikse, H. P. R. (1996). *CRC handbook of chemistry and physics : a ready-reference book of chemical and physical data* (75th edition ed.). CRC.

Mitchell, J. K. (1976). *Fundamentals of soil behavior*. Wiley. http://www.gbv.de/dms/bowker/toc/9780471611684.pdf

Spagnoli, G. (2021). *A review of soil improvement with non-conventional grouts*. Taylor & Francis. https://doi.org/10.1080/19386362.2018.1484603

Suelen da Rocha Gomes, L. F., Luis Sánchez, Mercedes Sánchez Moreno. (2023). A comprehensive review of cementitious grouts: Composition, properties, requirements and advanced performance. *Construction and Building Materials*, *375*, 130991. https://doi.org/ 10.1016/j.conbuildmat.2023.130991

Verma, H., Ray, A., Rai, R., Gupta, T., & Mehta, N. (2021). Ground improvement using chemical methods: A review. *Heliyon*, *7*(7). https://doi.org/10.1016/j.heliyon.2021.e07678

Walker, A., Kartofilis, D., & Pearlman, S. (1997). *Advances in grouting technology*. The mining journal Ltd.